JOURNAL OF MATERIALS SCIENCE 24 (1989) 2594–2602

Fracture of Al–4% Cu–0.1% Fe single crystals

G. GONZÁLEZ-DONCEL, M. TORRALBA, O. A. RUANO
Centro Nacional de Investigaciones Metalúrgicas, C.S.I.C. Av. Gregorio del Amo 8, 28040 Madrid, Spain

The fracture behaviour of heat-treated Al–4% Cu–0.1% Fe single crystals was studied in tension at room temperature. Three heat-treatment conditions were examined: quenched, fully hardened and overaged. Slip lines, shear bands and fracture surfaces were studied to yield information on the plastic deformation processes occurring prior to fracture. The presence of stable Al_7Cu_2Fe particles was found to be an important factor in fracture formation. In the as-quenched condition two fracture planes of different topography were formed. Large shear zones together with scattered shallow dimples were observed in both planes due to stable particles. In the fully hardened condition fracture occurred without necking and usually by shearing along the conjugate slip system. The presence of shear zones and dimples of different sizes was observed. Finally, in the overaged condition fracture took place by void coalescence after strong necking, as in polycrystalline samples. No shear zones were observed on the fracture surface of these samples.

1. Introduction

Single crystal mechanical behaviour of Al–Cu alloys has often been investigated in order to understand the elementary dislocation processes that govern deformation. It is well known that deformation of face centred cubic (fcc) single crystals occurs by slip on a $\{1\,1\,1\}$ plane in a $\langle 0\,1\,1\rangle$ direction. As slip proceeds on the primary system, the tensile axis of the sample rotates toward the $[\bar{1}\,0\,1]$ direction, which may allow another system to operate (usually the conjugate) [1]. Single crystal studies facilitate the determination of localized modes of deformation, such as necking or shear band formation, depending on the ageing condition.

There have been extensive studies on the plasticity of Al–Cu alloy single crystals, including slip line and shear band formation previous to fracture in different stages of ageing [2–8]. However, much less investigated is the fracture behaviour of samples tested under various heat treatments and some disagreement exists in the literature, especially in regard to the fully hardened condition.

Dew-Hughes and Robertson [4, 5] studied the fracture of hardened Al–4% Cu single crystals containing Guinier–Preston (G–P) zones and θ'' phase. According to these authors, fracture takes place on the primary (1 1 1) slip plane after considerable deformation in a narrow band and is a shearing process in which real crack initiation does not take place.

Beevers and Honeycombe [3] investigated single crystals of an Al–5% Cu alloy aged to maximum hardness to contain G–P zones and θ'' phase. They found that single or multiple slip occurred depending on the crystal orientation and the amount of rotation during deformation. The fracture of those crystals, with initial orientations distant from the [0 0 1]–$[\bar{1}\,1\,1]$ symmetry boundary, took place without necking on the primary slip system before the sample axis reached the boundary. On the other hand, duplex slip was observed when the symmetry boundary was reached and fracture occurred parallel to one of the operative slip planes, usually the conjugate system. Later, the same authors assumed that fracture developed along the primary slip plane and sought an explanation in terms of nucleation of cracks by dislocations [6]. They also investigated fracture of single crystals oriented close to the $[\bar{1}\,1\,1]$ corner of the stereographic triangle and found that fracture occurred on the (0 0 1) planes.

Price and Kelly [7] investigated the fracture of Al–3.7% Cu fully hardened single crystals and found that fracture took place on a $\{1\,1\,1\}$ plane in a work-hardened zone of the sample. The fracture occurred without necking and three stages were observed: (i) shear band formation, (ii) localized shearing within one band, and (iii) final separation by propagation of a crack across the sheared band by coalescence of voids. The slip bands usually formed on the conjugate slip system when the specimen axis overshot the symmetry boundary, or on the primary system when axis rotation was small. However, when axis rotation was small, it was not clear whether the specimen axis reached the symmetry boundary or not.

From these investigations, it can be inferred that the fracture behaviour of Al–Cu single crystal alloys is not completely understood and that more experiments should be conducted.

More recently, shear bands have drawn attention because of their importance in the deformation and failure of Al–Cu alloys [9–11]. The formation of coarse slip bands, aligned with the active slip systems, have been correlated with a critical slip plane strain-hardening rate. Chang and Asaro [9] studied the shear localization behaviour of single crystals containing θ, θ' and θ'' particles. They found that the shear bands

0022–2461/89 $03.00 + .12

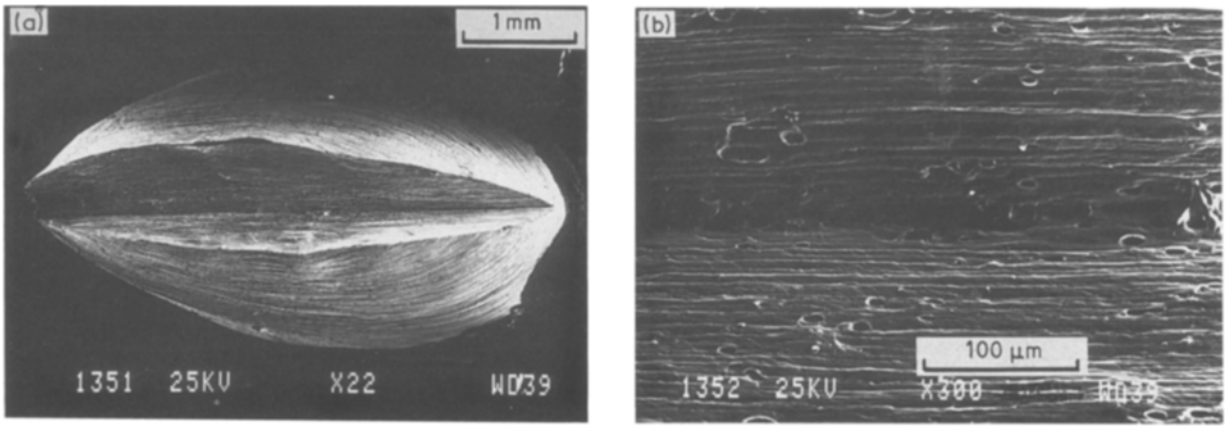

Figure 1 Top view of the fracture in the as-quenched condition. (a) The "double wedge" formation characterized by two facets and an intersecting line. (b) Slip lines and cavities formed on the internal facets on both sides of the intersecting line situated in the centre of the figure.

were not parallel to the active slip systems but were misaligned by several degrees. The crystalline planes within the bands were rotated away from the tensile axis, which may have led to a geometrical softening in agreement with the model suggested by Saimoto *et al.* [12].

In the present paper, the fracture behaviour at room temperature of Al–4% Cu–0.1% Fe single crystals in the fully hardened condition and in two other stages of ageing was studied. Special emphasis was made in the analysis of slip lines, shear bands and fracture planes. In order to establish the crystallographic planes and directions involved in the deformation process prior to fracture, the diffractometer method was used. This method maintains the relative orientation of the single crystal, both before and after deformation, and allows the crystallographic planes on which fracture occurs to be easily determined. At the same time, the technique compares favourably with the Laue back-reflection method when the orientation of deformed single crystals is to be measured [13].

2. Experimental procedure

An Al–Cu-based alloy was cast, then extruded at 530° C to 7 mm rods. The chemical analysis of the alloy gave the following composition: Cu 4.0, Fe 0.1, Zn 0.02, Si 0.08, Mn < 0.01, Mg < 0.01, Pb < 0.01, Cr < 0.01, Ni < 0.01, Al balance.

The extruded material was recrystallized at 540° C for 20 min to a fine and homogeneous grain size of about 100 μm. Single crystal rods, of 7 mm diameter and about 300 mm long were then grown by the strain-anneal method. The orientations of the rod axes were randomly distributed in the stereographic triangle. Tensile samples with a 30 mm gauge length and a 5.5 mm diameter were machined from the single crystals. Orientations distant from the corners of the stereographic triangle were chosen and a few tensile tests with orientations next to the $[\bar{1}\,1\,1]$ corner were conducted.

A solid solution treatment of 2 h at 540° C followed by water quenching to room temperature was carried out. The samples were then tested in three different ageing conditions which were followed by hardness measurements [14]: (1) as-solution treated; (2) aged at 150° C for 100 h to obtain a fully hardened condition; (3) aged at 350° C for 100 h to approach equilibrium (overaged condition).

Optical and scanning electron microscopy were used to study slip bands and fracture surfaces. Second-phase particles were examined by microprobe analysis.

Prior to testing, the crystals were electropolished in a solution of two parts of methanol and one part of nitric acid for macroscopic observation of slip lines. Tensile tests were carried out on an Instron electromechanical testing machine at room temperature at an initial strain rate of $9.5 \times 10^{-4}\,\mathrm{sec}^{-1}$.

The orientation of the crystals was determined by the diffractometer method using Cu$K\alpha$ radiation.

3. Results and discussion

Microprobe analysis of the alloy revealed the presence of non-soluble particles of the ternary phase Al_7Cu_2Fe in all three conditions. The particle size ranged from less than 1 μm to about 10 μm. Small particles were round and large particles were elongated in shape. In the overaged condition the alloy revealed, in addition, round particles of the binary phase Al_2Cu of about 2 μm.

The occurrence of fracture and the appearance of the fracture surface was markedly dependent on ageing conditions. This is due to the different precipitation stages of copper in the aluminium matrix. The presence of non-soluble particles of the ternary phase Al_7Cu_2Fe was always detected on the fracture surface of all samples tested at the different ageing conditions.

3.1. Quenched crystals

Fracture of tensile samples tested in the as-quenched condition was characterized by the formation of a "double wedge". The macroscopic appearance of this type of fracture is the same as that of pure f c c single crystals, as has been previously reported in the literature [15, 16]. This fracture was observed by Beevers and Honeycombe [3] in Al–4% Cu single crystals under the same heat treatment and was named the "crocodile type" of fracture.

An example of the "double wedge" formation obtained can be seen in the low magnification

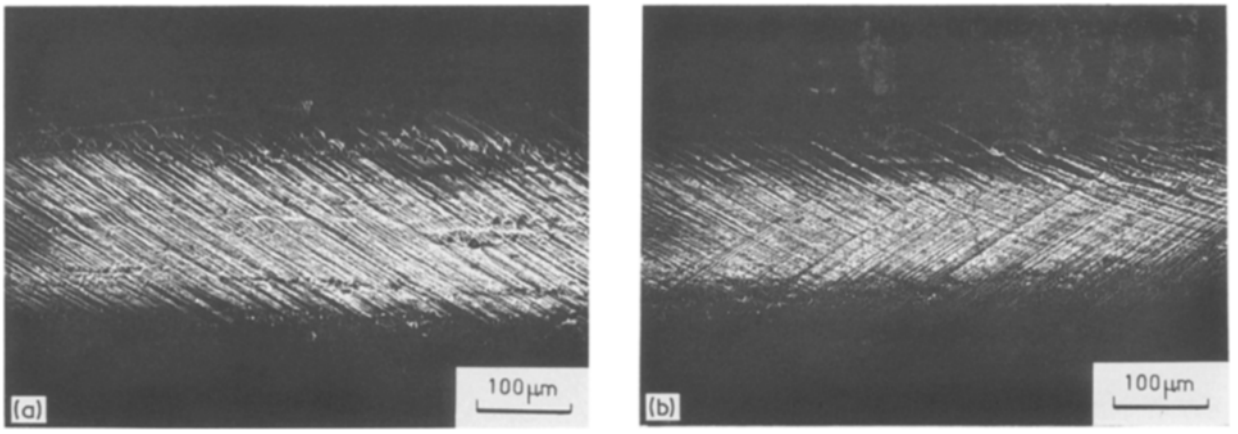

Figure 2 Appearance of slip lines on the gauge length of a sample tested to fracture in the as-quenched condition. (a) Slip lines of the primary system in a region away from the fracture. (b) Slip lines of the primary and conjugate systems in a region close to the fracture.

micrographs of Fig. 1. Both parts of the sample that result after separation (Fig. 1a) are identical. Their formation will be discussed later. The fracture surface is characterized by the presence of two flat facets intersecting in a line that can be seen at the bottom. Each facet contains a set of slip lines parallel to the intersecting line (see Fig. 1b). This figure is a magnified micrograph of the central region of Fig. 1a. Slip lines are also shown in Fig. 1a on the external surface of the sample. Cavities due to the presence of iron-containing second-phase particles may also be observed in Fig. 1b. The effect of these particles on the facet appearance of the "double wedge" was very small. Although some voids are present, the lines remain straight and parallel to each other indicating that the slip occurred as though particles were not present.

The "double wedge" formation is due to simultaneous activation of two different systems: the primary and the conjugate slip systems. Single-crystal deformation starts on the primary slip system causing the appearance of slip lines throughout the sample (Fig. 2a). Crystals would tend to rotate their axes so that two slip systems would become geometrically equivalent. Deformation proceeds, then, by slip on both systems in a restricted region (≈ 8 mm) of the sample (Fig. 2b). This figure shows typical slip lines arising from extensive duplex slip. The density of the lines corresponding to the conjugate slip system increases in the necked region on the right of the figure where fracture takes place.

Each set of slip lines contained on both facets of the fracture surface (Fig. 1) is the result of slip on one of the slip systems. In other words, each of the two facets corresponds to deformation on either the primary or conjugate slip systems. The intersecting line at the bottom of the fracture is, then, parallel to a $\langle 0\,1\,1 \rangle$ direction which is a direction defined by the intersection between $\{1\,1\,1\}$ slip planes. This statement can also be inferred from the micrographs of Fig. 3 which correspond to a different sample tested at the same heat treatment. Fig. 3a is a lateral view of the sample close to the fracture region and Fig. 3b is a magnified region next to the facets intersection. The upper left region of Fig. 3a corresponds to one of the facets of the "double wedge", that is, the fracture surface. The remaining three regions are part of the external surface on which slip lines can be appreciated. The upper right and lower left sheared regions belong to each of the wedges formed. The lower right region corresponds to a surface away from the sheared zone. The intersecting line of the two facets is also shown in this figure as the separation between the upper and lower left regions of the micrograph. Fig. 3b is a magnified region close to the centre of Fig. 3a. On the right side of this micrograph, which is the region away from the sheared zone, slip lines of the primary slip system can

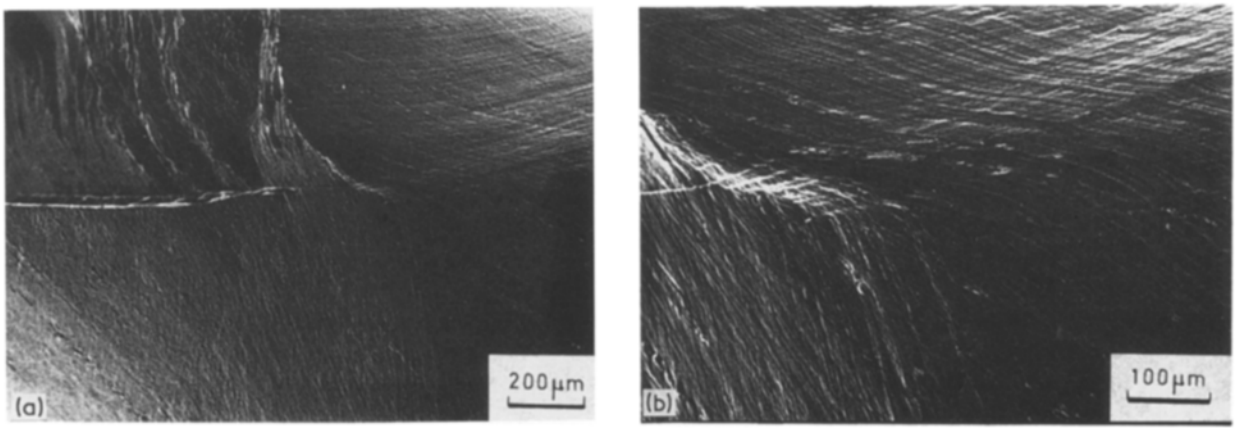

Figure 3 Lateral view of the fracture region of a sample tested in the as-quenched condition. (a) Intersection of primary and conjugate slip systems in the centre of the figure. (b) Magnified micrograph showing details of slip lines of both primary and conjugate systems.

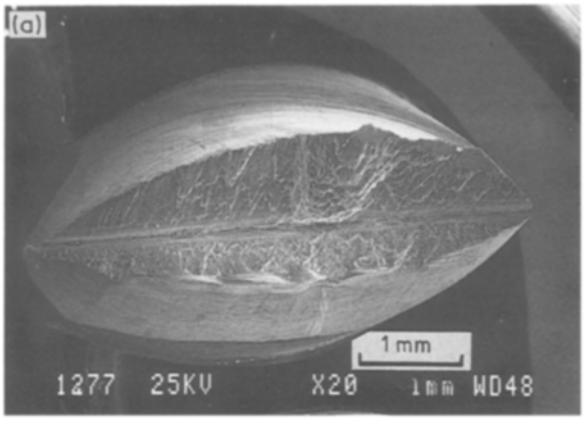

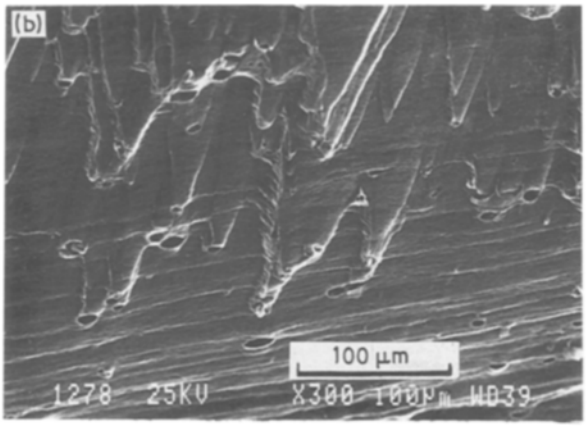

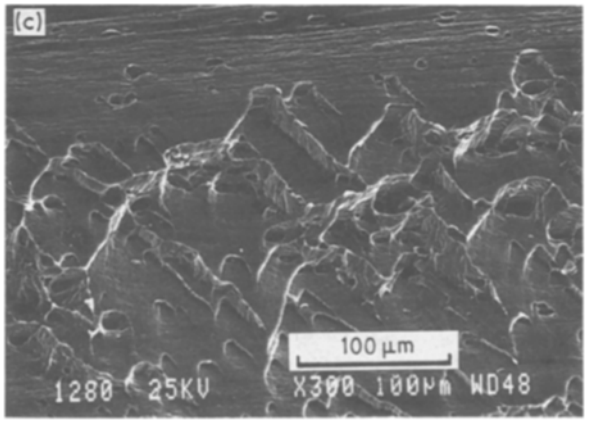

Figure 4 Top view of the fracture surface in the as-quenched condition. (a) General view of the fracture. (b) Slip lines and swallow dimples on the top facet. (c) Dimple formation at the iron-containing particles.

be appreciated. These lines arise from deformation of the single crystal by slip on the primary system before the necked region was formed. On the top region, which is one of the two sheared zones, lines from both slip systems are present. Those from the primary slip system originated before the sheared band was formed. The lines of the conjugate system determine the shear band that produced one of the wedges as explained by Saimoto *et al.* [12]. On the lower left part of the micrograph, extensive shearing from the primary slip system, which produced the other wedge, is observed. The misalignment between the slip lines of the primary system and those from the sheared region has also been observed by Chang and Asaro [9]. Finally, the intersection of slip lines from both sheared zones is observed on the left side of the micrograph. This interaction determines the origin of a quadrangular cavity which upon further extension will result in the "double wedge" formation [12]. This is an indication that the intersecting line is formed by double slip on both operative slip systems. It is clear, then, that the intersecting line of Fig. 1 is parallel to a $\langle 0\,1\,1 \rangle$ direction.

The rather flat fracture surface appearance shown in Fig. 1 is common to many pure single crystals and is present in about 10% of the single crystals studied in this investigation. The effect of iron-containing particles, however, is important in most cases. As can be observed in Fig. 3a, the appearance of the fracture surface is different from that of Fig. 1a. Typical fracture surfaces of these samples are shown in Fig. 4. Fig. 4a shows a low-magnification micrograph of the "double wedge" type of fracture of most samples tested under the supersaturated solid solution. Figs 4b and c are higher magnification micrographs of each facet on regions close to the intersecting line. As in Fig. 1a, considerable necking on the sample of Fig. 4a is apparent. A flat region corresponding to the upper facet next to the intersecting line can be seen in the higher magnification micrograph of Fig. 4b. This figure also shows some scattered voids, which are the origin of shallow shear dimples due to the presence of Al_7Cu_2Fe particles. Slip steps which are parallel to the intersecting line are also observed. The lower facet, shown in Fig. 4c, also reveals a flat region next to the intersecting line and the presence of more clearly defined dimples starting at microvoids that arise from the iron-containing particles (Al_7Cu_2Fe). The facet's roughness was not associated with slip on the primary or conjugate systems. The initiation of the "double wedge", i.e. the intersecting line and the quadrangular cavity formation, is due to pure shear for both samples described in Figs 1 and 4. The different fracture surfaces observed between both samples arise from different modes of deformation. Whereas in the example of Fig. 1 pure shear on each slip system is responsible for the "double wedge" formation, in most cases (Fig. 4), shearing and void formation, due to the presence of Al_7Cu_2Fe insoluble particles, are coupled processes that give rise to the roughness of the fracture surface.

3.2. Fully hardened crystals

Fig. 5 corresponds to the fracture surface of a single crystal tested in the fully hardened condition. As mentioned above, the macroscopic aspect of the fracture differs from that of the supersaturated solid solution. Necking is not observed in Fig. 5 and the fracture surface is rather flat. Some slip lines, parallel to the fracture surface, are also visible at the right of the figure.

The deformation process prior to fracture of samples tested in the fully hardened condition was the same as that for the supersaturated solid solution. In other words, slip occurred on the primary system causing a rotation of the tensile axis. In this case, however, when

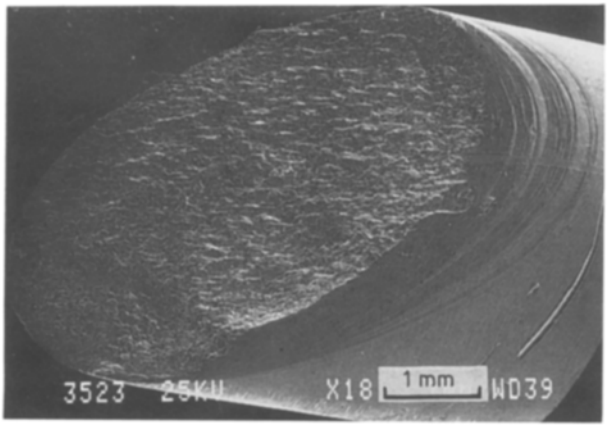

Figure 5 Fracture of a sample in the fully hardened condition.

the conjugate slip system became geometrically equivalent, this second slip system started to operate and a shear band of conjugate slip on a narrow zone was formed indicating the beginning of fracture. Deformation continued by shearing on this band, and shortly thereafter fracture occurred. This behaviour is shown in Fig. 6. Two sets of slip lines that were the result of the activation of two different slip systems are clearly defined. The slip lines distributed throughout the sample belong to the primary slip system and the localized shear band in the centre of the figure resulted from the activation of the conjugate slip system on a narrow zone. The strong distortion observed on the slip lines of primary system on the intersection with the conjugate shear band reveals the extensive shearing process that occurred along this band. This behaviour was observed on most of the single crystal studied in this investigation. However, in some cases shear bands on the primary or even the cubic $(0\,0\,1)[\bar{1}\,1\,0]$ slip systems were also formed (see below).

These results are basically in agreement with those of Price and Kelly [7] except that they observed coarse band formation on the primary slip system only when axis rotation is small (i.e. fracture along primary slip systems occurs only when the specimen axis is distant from the symmetry boundary). In contrast, our tests showed that fracture along the conjugate slip system occurred independently of the amount of axis rotation and always when the tensile axis was in the vicinity of the symmetry boundary; sometimes after a small overshooting of less than two degrees. The localized shear band observed in this investigation is very similar to the macroscopic shear band described by Price and Kelly [7] and by Chang and Asaro [9]. However, in the present work it was not possible to define clearly the difference between slip lines and coarse slip bands as done by these authors. For this reason, only differences between slip lines and macroscopic shear bands will be noted.

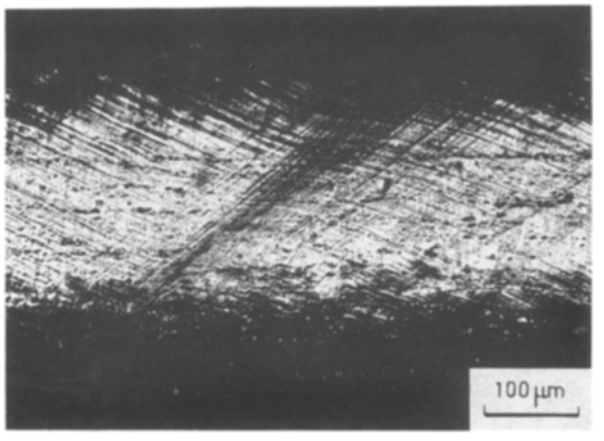

Figure 6 Beginning of fracture by shearing along the conjugate slip system of a sample tested in the fully hardened condition.

The explanation for the difference in fracture behaviour between the as-quenched and fully hardened conditions is based on the different states of precipitation. In the as-quenched condition, once the tensile axis reached the symmetry boundary, both slip systems operated simultaneously. Double slip continued practically until the end of the test and was responsible for necking and the "double wedge" type of fracture. In the fully hardened condition, however, once double slip started, fracture took place without necking by shearing along the conjugate slip system. The strong stress fields, created principally by shearing of primary slip system dislocations through the precipitates, represent an important obstacle for the motion of dislocations on the conjugate slip system because they also have to shear the particles. This cutting phenomenon is not present in the as-quenched condition where dislocations must only overcome the stress fields created by the solute atoms of copper. Hence, deformation of single crystals in this condition occurs as in a pure fcc single crystal.

Dew-Hughes and Robertson [4, 5] suggested that deformation in a narrow band is due to particle shearing, resulting in the development of a weakened plane in the crystal. This would not explain, however, why a shear band on the conjugate slip system was formed during the operation of the primary slip system (Fig. 6). On the other hand, Chang and Asaro [9] estimated the strain hardening in the bands and found an increase in the shear stress on the plane of the band and in the shearing direction thus excluding the development of weakened planes. These authors gave an explanation of shear band formation preceding fracture, after the work of Saimoto *et al.* [12], based on geometrical softening. This argument is based on the observation that the operative slip plane in the band parallel to the primary and conjugated slip planes is rotated away from the tensile axis.

A misalignment between the fracture surface originated by the shear band and the active slip systems was also measured in the present work. In Fig. 7, the crystal rotation of the tensile axis relative to the crystal for an fcc structure is represented on a stereographic projection. The tensile axis, A, is shown in the stereographic triangle $[0\,0\,1]$–$[0\,1\,1]$–$[\bar{1}\,1\,1]$. As deformation starts on the primary slip system, $(1\,1\,1)[\bar{1}\,0\,1]$, point A changes in orientation to A′ (dotted line). In this figure, α represents the angle between the normal to the slip plane of the slip system associated with the fracture surface and the single crystal tensile axis when the symmetry boundary is reached. It is also possible to define an angle β between the tensile axis and the normal to the fracture surface itself. Finally, γ is defined as the angle between the fracture surface and

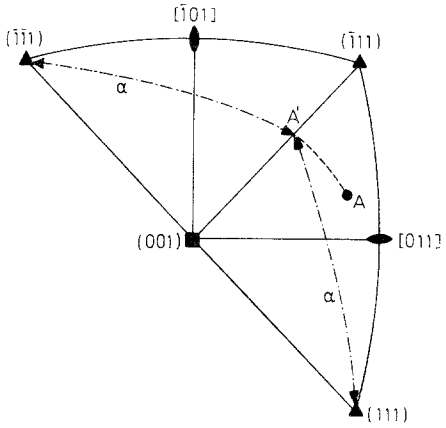

Figure 7 Rotation of the tensile axis and determination of angles involved in the fracture formation of a sample tested in the fully hardened condition.

the slip plane responsible for the shear bands generated prior to the fracture and is the difference between α and β.

Table I shows the angles α and β that determine the fracture geometry for two differently oriented single crystals. Two samples with the same orientation were obtained from each single crystal. All samples fractured when the final orientation of the tensile axis was within two degrees of the symmetry boundary. The slip system on which fracture occurred is also indicated. The table shows positive values of γ, between 6° and 13°, that is, α is always larger than β, indicating a misalignment between the fracture surface and the corresponding slip system. This behaviour is not a function of the initial orientation, i.e. it was not observed in crystals with different degrees of rotation. Also, the misalignment observed was independent of the slip system in which fracture occurred.

TABLE I Angles determining the fracture geometry

	Single crystal 1		Single crystal 2	
	Sample (a)	Sample (b)	Sample (c)	Sample (d)
Plane of fracture*	P	C	P	C
α	63	63	57	57
β	51	57	46	44
γ	12	6	11	13

*P, primary; C, conjugate.

As mentioned above, most of the crystals in the fully hardened condition fractured by shear bands corresponding to the conjugate slip system. There are some exceptions, however, to this general behaviour. Fig. 8 corresponds to a crystal that fractured by shear band formation on the primary slip system. The fracture surface of the crystal is at the right of the micrograph of Fig. 8a. A strong shear band from the conjugate slip system, which was the system where fracture initiated, is apparent in the centre of the figure. The intersection of this shear band (running from left to right) with the slip lines from the primary slip system can be observed at higher magnification in the micrograph of Fig. 8b. The steps produced on the slip lines of the primary slip system by the conjugate slip band are easily recognized. Fig. 8c shows the region where the shear band encounters a small grain located on the surface of the gauge length of the sample. The hole formed by this grain can be seen at the top of the micrograph. We assume that this grain stopped further development of the shear band allowing the

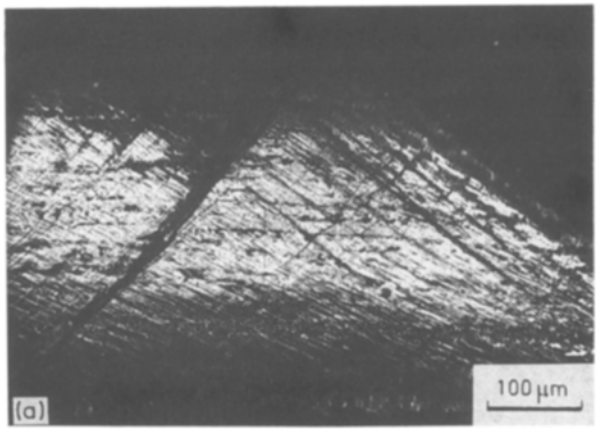

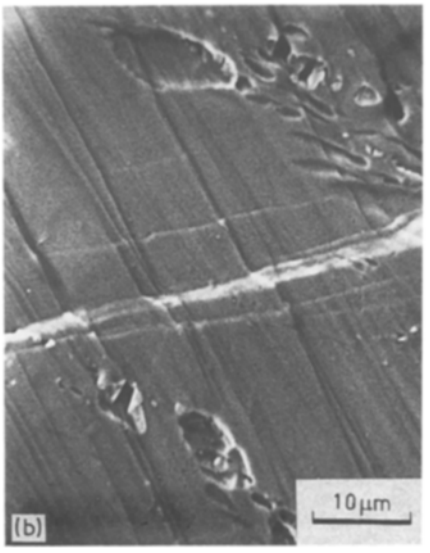

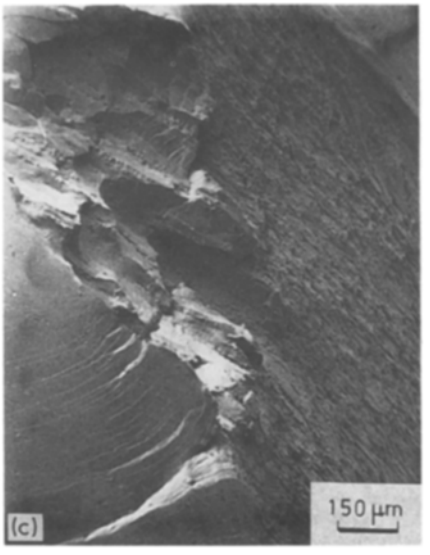

Figure 8 Fracture of a sample along the primary slip system in the fully hardened condition. (a) Shear band formation along the conjugate slip system. (b) Steps on primary slip lines produced by the shear band. (c) Heterogeneity from a small grain on the surface of the sample and conjugate shear band at the bottom of the micrograph.

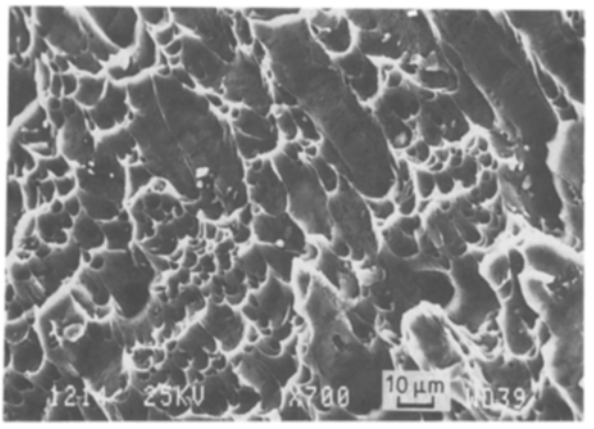

Figure 9 Fracture surface showing dimples and shear zones oriented along the shear direction on a sample tested in the fully hardened condition.

fracture process to proceed along the primary slip system.

Other crystals that fractured along the primary slip system showed small grains on the surface of the sample or some kind of heterogeneities. It is thus reasonable to think that these defects are responsible for the resistance to further development of shear bands because fracture by shearing along the primary slip system was observed on crystals with very different initial orientations.

Fig. 9 is a scanning electron micrograph of a typical fracture surface observed in the fully hardened condition. The micrograph shows the presence of flat regions associated with pure shear processes and dimple formation associated with the presence of Al_7Cu_2Fe particles. Shear regions and dimples are elongated along the slip direction of the system operative prior to fracture. Small dimples of about 3 to 5 μm diameter were formed around Al_7Cu_2Fe particles smaller than 1 μm and large dimples of about 10 μm were formed around particles larger than 5 μm that are visible on the micrograph. The fracture surface of crystals sheared along the primary slip system revealed the same aspect of flat shear regions and dimples as those fractured along the conjugate.

Fracture of some of the crystals oriented close to the $[\bar{1}\,1\,1]$ pole occurred on (0 0 1) cubic planes. This is because the proximity of the $[\bar{1}\,1\,1]$ pole allows several slip systems to be available. Fig. 10 shows the fracture of two samples obtained from the same single crystal oriented close to the $[\bar{1}\,1\,1]$ pole. Both samples are arranged to maintain the same orientation in this figure, i.e. with the semi-axes of the elliptical cross-section parallel to each other. In this manner, differences in the orientation of the fracture surface can be appreciated. Both crystals started deformation on the primary slip system. Once the $[0\,0\,1]$–$[\bar{1}\,1\,1]$ boundary was reached, a different shear band was formed on each sample. In the sample on the right, the conjugate slip system started acting and fracture occurred by shear on this system. In the sample shown on the left, after some deformation was achieved, slip lines from the cubic slip system appeared in a limited zone of the sample and fracture took place shortly after by shearing along the cubic $(0\,0\,1)[\bar{1}\,1\,0]$ slip system. Cubic

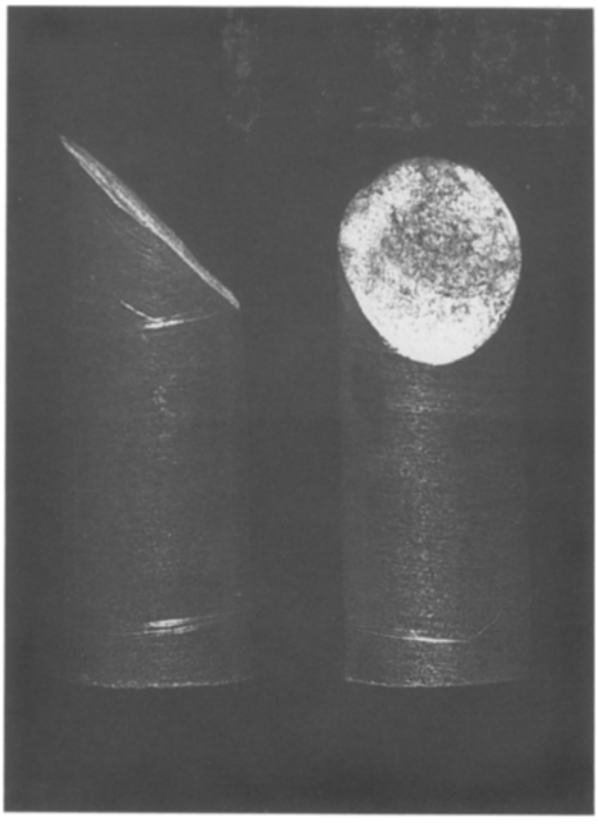

Figure 10 Fracture of samples along the conjugate (right) and cubic (left) slip systems in the fully hardened condition. Both samples had the same initial orientation with tensile axes close to the $[\bar{1}\,1\,1]$ corner of the stereographic triangle.

slip occurred on two out of eight single crystals with initial orientation close to the $[\bar{1}\,1\,1]$ pole. The fracture surface again showed the presence of shear dimples and shear zones similar to those described in Fig. 9.

Fracture by shear band formation along the cubic slip system has been previously observed by Beevers and Honeycombe [17] always on crystals closely oriented to the $[\bar{1}\,1\,1]$ pole. This is attributed to the favourable orientation of this slip system when the tensile axis of the crystals is near to the $[\bar{1}\,1\,1]$ pole. In our case, however, roughly 25% of these crystals fractured along the cubic slip system.

3.3. Overaged crystals

Fig. 11 corresponds to the fracture surface of a single crystal tested under the overaged condition. Although a strong necking as in the supersaturated solid solution is present, the macroscopic aspect is very different. The fracture is characterized by a cup and cone type of fracture similar to that observed in polycrystalline materials.

Fig. 12 is a scanning electron micrograph of the external surface on a region close to the fracture. In this figure Al_2Cu precipitates that were formed during the overageing heat treatment can be clearly seen. Some faint slip lines due to slip on several slip systems are also shown. These lines were only observed after extensive deformation. The fracture surface topography is shown in Fig. 13. The micrograph shows the presence of small (about 2 μm) equiaxed dimples due to Al_2Cu precipitates and some large dimples (about 10 μm) due to Al_7Cu_2Fe particles. Both kinds of

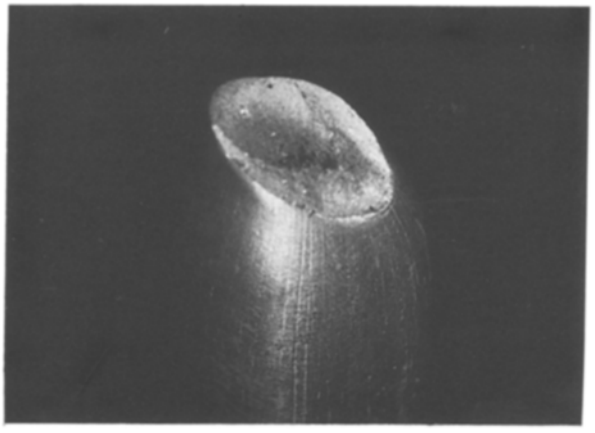

Figure 11 Fracture of a sample in the overaged condition.

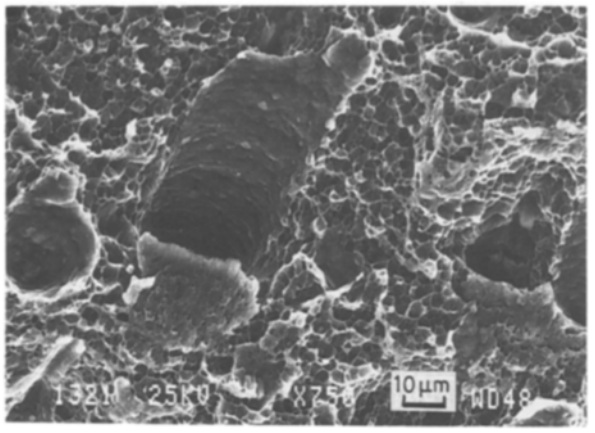

Figure 13 Fracture surface of a sample tested in the overaged condition. The small dimples are due to $AlCu_2$ precipitates and the large dimples are due to Al_7Cu_2Fe particles.

particle are often found at the bottom of the dimples. Unlike the other heat treatments, no shear bands could be found during the necking formation and no shear regions were observed on the fracture surface.

The fracture behaviour of tested samples under this heat treatment is characterized by simultaneous activation of several slip systems in the early stages of deformation. Moving dislocations on the primary slip system may overcome the stable Al_2Cu particles by the Orowan mechanism. This results in the activation of different slip systems almost simultaneously and, hence, in an extensive work hardening produced during tensile tests. For the same reason, neither shear regions nor slip directions are found on the fracture surface.

4. Conclusions

1. Single crystals of Al–4% Cu, containing 0.1% Fe, fracture in tension very differently depending on the heat-treatment condition.

2. In the solution-treated condition, the crystals developed clearly defined slip lines of the primary slip system. These lines were observed over the entire gauge length of the sample. Then, slip lines of the conjugate slip system appeared in a narrow zone of the gauge length. Finally, failure occurred by shear formation simultaneously on both slip systems. This gave a "double wedge" type of fracture with strong necking and the formation of two facets, generally with different topography. One of the facets had a smooth appearance with large shear areas and shallow shear dimples. The other facet was granulated with elongated shear dimples starting at Al_7Cu_2Fe particles.

3. In the fully hardened condition, the crystals tested fractured in the absence of necking. Deformation started by slip on the primary slip system and then localized shear on the conjugate slip system occurred and the crystal quickly fractured. Fracture by shearing on the primary slip system was observed when a heterogeneity was present in the crystal. Fracture by shearing on the cubic slip system was observed when the tensile axis was near the $[\bar{1}\,1\,1]$ pole. Fracture surfaces always showed the presence of shear zones and shear dimples that arose from voids created around small Al_7Cu_2Fe particles.

4. In the overaged condition, faint slip lines were observed only after considerable deformation. These lines corresponded to several slip systems that were almost simultaneously activated from the beginning of deformation. A "cup and cone" type of fracture similar to that of polycrystalline materials was observed. The fracture surface showed the presence of small (about 2 μm) non-elongated dimples due to Al_2Cu precipitates, and large (about 10 μm) dimples due to Al_7Cu_2Fe particles which were found at the bottom of the dimples. No shear zones were found indicating that only void coalescence caused fracture.

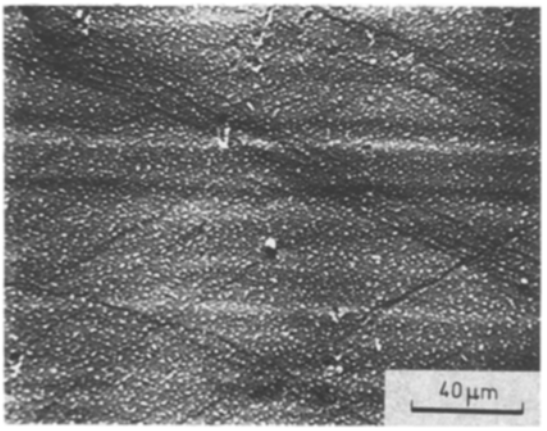

Figure 12 Appearance of slip lines between Al_2Cu precipitates on a sample tested in the overaged condition.

References

1. C. N. REID, "Deformation Geometry for Material Scientist" (Pergamon Press, Oxford, 1973).
2. K. M. CARLSEN and R. W. K. HONEYCOMBE, *J. Inst. Metals* **83** (1954–55) 449.
3. C. J. BEEVERS and R. W. K. HONEYCOMBE, in "Fracture", edited by B. L. Avervach, D. K. Felbeck, G. T. Hahn and D. A. Thomas (Wiley, New York, 1959) p. 474.
4. D. DEW-HUGHES and W. D. ROBERTSON, *Acta Metall.* **8** (1960) 147.
5. *Idem, ibid.* **8** (1960) 156.
6. C. J. BEEVERS and R. W. K. HONEYCOMBE, *ibid.* **10** (1962) 17.
7. R. J. PRICE and A. KELLY, *ibid.* **12** (1964) 979.
8. M. TORRALBA and G. WASSERMAN, *Z. Metallkde* **59** (1968) 467.
9. Y. W. CHANG and R. J. ASARO, *Acta Metall.* **29** (1981) 241.

10. K. MORII and Y. NAKAYAMA, *Scripta Metall.* **20** (1986) 1237.
11. K. MORII, H. MECKING and Y. NAKAYAMA, *Acta Metall.* **33** (1985) 379.
12. S. SAIMOTO, W. F. HOSFORD and W. A. BACKOFEN, *Philos. Mag.* **12** (1965) 319.
13. G. GONZALEZ, M. TORRALBA and O. RUANO, Proceedings of 6th Asamblea General CENIM, Madrid (1985).
14. G. GONZALEZ, PhD dissertation, Universidad Complutense de Madrid, Madrid (1986).
15. C. F. ELAM, *Proc. Roy. Soc. A* **109** (1927) 143.
16. R. KARNOP and G. SACHS, *Z. Phys.* **41** (1927) 116.
17. C. J. BEEVERS and R. W. K. HONEYCOMBE, *Acta Metall.* **9** (1961) 513.

Received 29 April
and accepted 9 September 1988